ICWE14
June 21-26, 2015 | Porto Alegre - Brazil
14th INTERNATIONAL CONFERENCE ON WIND ENGINEERING

Experimental Validation of the Wing-Aileron-Tab Combination Applied to an Actively Controlled Bridge Section Model

Maria Boberg[1,2], Glauco Feltrin[1], Alcherio Martinoli[2]
[1]Structural Engineering Laboratory, Swiss Federal Laboratories for Materials Science and Technology, Duebendorf, Switzerland
[2]Distributed Intelligent Systems and Algorithms Laboratory, School of Architecture, Civil and Environmental Engineering, École Polytechnique Fédérale de Lausanne, Switzerland
email: maria.boberg@epfl.ch, glauco.feltrin@empa.ch, alcherio.martinoli@epfl.ch

ABSTRACT: In this work we investigate the applicability of the wing-aileron-tab model for a bridge section model being actively controlled with leading and trailing edge flaps. The structural and aerodynamic model parameters have been extracted experimentally from a total of 140 wind tunnel experiments. Our in-house developed set-up has been employed for this purpose. Four different control strategies, with increasing complexity have been used for the parameter estimation. The first eight flutter derivatives have been obtained from step responses performed without control. The modified versions of these flutter derivatives have been estimated from step responses performed with three different types of active flap control, from which the leading edge and trailing edge flutter derivatives have been derived. The presented results are encouraging, however, further investigation is necessary in order to fully evaluate the wing-aileron-tab model's applicability.

KEY WORDS: Wind actions and effects on long-span bridges; Mitigation of Wind-Induced Vibrations; Wind Tunnel Tests; Wind-Structure Interaction; Bridge Flutter; Active Flutter Control; Control Flaps.

1 INTRODUCTION

Long-span bridges are particularly vulnerable to wind loads, owing to their inherently low structural damping, low natural frequencies, and adjacent fundamental torsional and vertical mode frequencies. This leads to wind-induced instabilities, causing potential damage to the whole structure.

Most solutions for this problem deployed on real bridges consist of passive elements that reduce the aerodynamic requirements on the cross-section (e.g., streamlining the deck profile) [1]. However, a passive solution cannot adapt to dynamic wind conditions. Active solutions could potentially lead to a more favorable performance/cost trade-off in the building and maintenance phases as well as new opportunities for improving bridge aesthetics.

One possible active solution is to install multiple mobile flaps along the bridge girder in order to alter its aerodynamic profile, enabling stabilizing forces on the structure, a concept illustrated in Figure 1. Furthermore, the angular position of the adjustable flaps is controlled as a function of the wind field and/or the displacement of the structure whose dynamic state can be measured with an underlying sensor network.

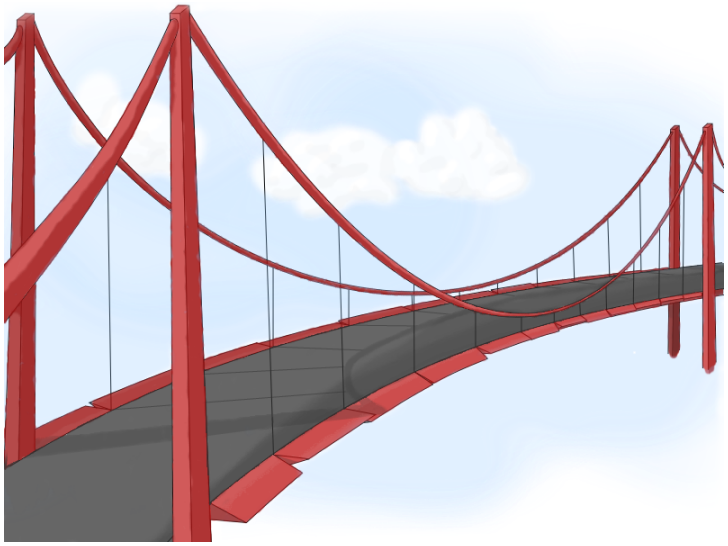

Figure 1: Conceptual figure of the multi-flap wind mitigation strategy.

Different approaches to controlling the flaps have been investigated in literature, where the biggest distinction is between passively and actively controlled flaps. Although, both strategies have to some extent been proven efficient for controlling bridge deck flutter, both in theory and in practice, the passive solution has a general practical disadvantage: once the experimental set-up is implemented, cumbersome and time-consuming procedures are required for tuning the control parameters and in turn the system response, since the components need to be changed physically, whereas active control parameters are easily adjusted through software modifications.

While the use of moving flaps to dampen bridge deck oscillations has been investigated theoretically, particularly with respect to the flutter phenomenon, only a handful of research groups have provided experimental validation of bridge flutter control. Kobayashi et al. were the first to implement actively controlled flaps on a bridge deck in order to stabilize flutter. In [2] they constructed a section model with flaps installed above the bridge deck and in [3] they instead attached the flaps at the deck level. The flaps were controlled as a function (amplitude gain and phase shift) of either the deck's heave or pitch. In both works they showed that they can efficiently suppress flutter (flutter wind speed increased by 50%) with wind tunnel experiments. Their aerodynamic model is based on Theodorsen's circulatory function for thin airfoils [4] and is extended with a modified version of the wing-aileron-tab configuration (changed to bridge deck with leading and trailing flaps) developed by Theodorsen and Garrick [5], as shown in Figure 2. The structural dynamics are modeled in two dimensions (heave and pitch) as two uncoupled harmonic oscillators, where the mass and moment inertia of the deck is considered (aileron mass is assumed to be zero). However, the experimental and theoretical results (flutter always suppressed) did not match well, a fact that the authors mainly attributed to the occurrence of torsional divergence, an effect that was not taken into account in their model. Hansen et al. also designed a bridge deck capable of stabilizing the bridge vibrations, with actively controlled flaps attached to the deck using a similar control approach [6]. Furthermore, they used the same approach as Kobayashi et al. to model their system. They also reported problems in verifying their model because the torsional divergence wind speed was too close to the flutter wind speed. Wilde et al. proposed a pendulum solution for passively actuating flaps, and were able to increase the flutter wind speed by 57% experimentally [7]. However, the experimental and analytical (based on the same theory as Kobayashi et al.) results only concurred for very small gain values; authors hypothesized that this discrepancy was because the aerodynamic forces of the system were not modeled correctly. Starossek et al. designed a system with passively controlled flaps using Tuned Mass Dampers (TMDs) [8]. They also showed experimental results with increased deck vibration damping using controlled flaps. Their design was based on the same theory of the wing-aileron-tab combination, however, they did not disclose a comparison between experimental and theoretical results. Kwon et al. designed passively actuated control surfaces using TMDs [9]. The control surfaces were significantly different from the solutions presented above: their flaps were not controllable in their angular position, but consisted rather of rectangular surfaces that moved in and out of slots from the bottom of the deck. They achieved an increase of the flutter wind speed by 43% with the TMDs augmented by the corresponding control surfaces. It is worth noting that using only the TMDs (control surfaces removed) they achieved a 37% increase of the flutter wind speed, a result that indicates that the added wind-mitigation impact of their control surfaces was minimal. They included the mass and mass moment inertia of the control elements in their structural model, while their aerodynamic model was based on the classical Theodorsen theory (control surfaces were disregarded as the wing-aileron-tab combination was not applicable). Consequently, they showed a very good relation between the experimental and analytical result for the flutter control using only TMDs, and a large discrepancy for the flutter control using TMDs and control surfaces.

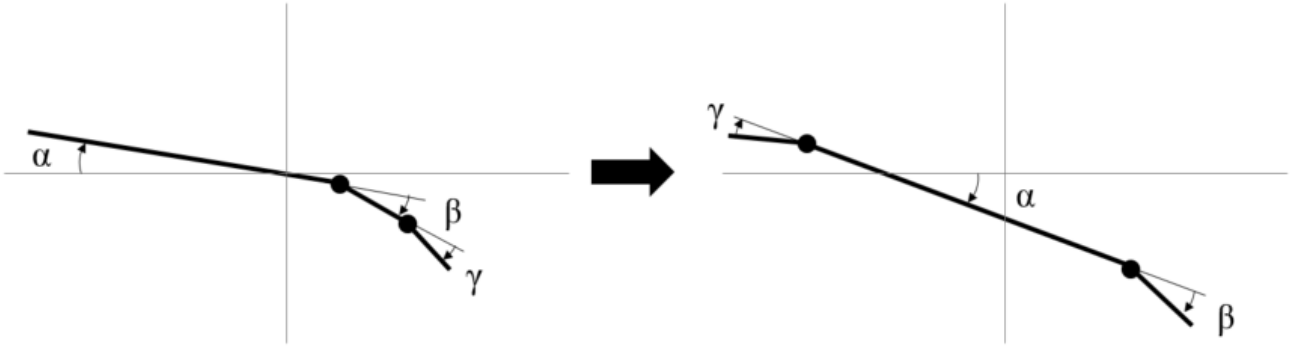

Figure 2: The wing-aileron-tab combination and the transformation to a bridge deck with leading and trailing flaps.

In summary, all the prior experimental work investigating flutter suppression with flaps based their analytical model of the aerodynamic forces on a modified version of the wing-aileron-tab combination (except for Kwon et al. [9], where this model was not applicable). However, since all these contributions represent pioneering efforts to investigate experimentally solutions involving mobile control surfaces, the focus has mainly been on achieving flutter suppression and thus validating the concept and design. The model has primarily been leveraged for the initial design of the control law, and no real effort has been put on validating the model with experimental results. We believe that a key factor for the reported discrepancies between the experimental and theoretical results is that most of the model parameters (structural and especially aerodynamic) were calculated theoretically and not directly estimated from the experimental set-up. A few of the above mentioned works did attempt to estimate some of the model parameters experimentally; however, to few details on the methods selected and resulting quality of the results are reported. For instance, Kobayashi et al. mentioned estimation of experimental aerodynamic model parameters [3], however, it was not disclosed exactly which ones were estimated nor the estimation procedure. Furthermore, Wilde et al. used experimentally extracted aerodynamic model parameters, however, only for the fixed deck, i.e. ignoring the flaps [7]. Finally, although Kwon et al. did not explicitly include the control surfaces in their aerodynamic model, they did attempt to capture the effect of the control surfaces by estimating a few of the aerodynamic parameters experimentally (while the deck was being

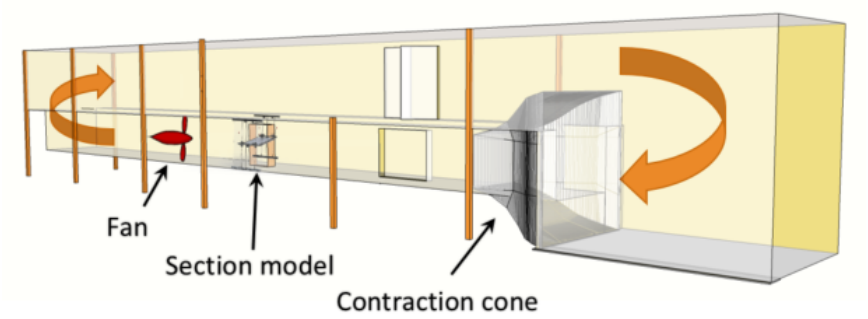

Figure 3: The wind tunnel and set-up.

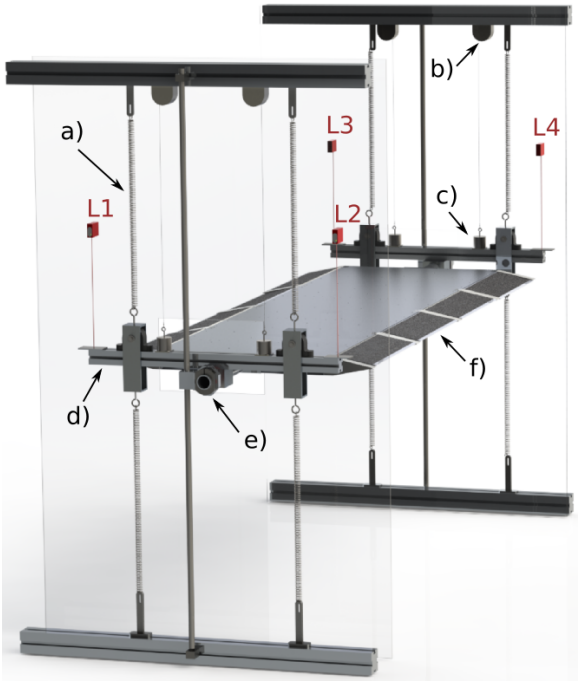

Figure 4: The SmartBridge anchored to the suspension system. Some key elements of the set up are highlighted in the figure: a) spring for the suspension system, b) DC motor for the pull-up system, c) electromagnet for the pull-up system, d) support bar, e) decoupling system, and f) active flap. Moreover, four laser sensors are measuring the corner positions of the deck and are marked with L1-4.

controlled) using local pressure measurements [9]. Although Hansen et al. did not estimate aerodynamic model parameters they did perform a thorough experimental investigation of the structural model parameters [6]. The heave and pitch natural frequencies, as well as the pitch damping, were determined experimentally with and without moving flaps under varying wind conditions.

In this work, we aim to thoroughly investigate the applicability of the wing-aileron-tab combination to a bridge deck equipped with moving leading and trailing edge flaps. We will conduct systematic experiments in order to estimate all the model parameters. In order to do so we will leverage the experimental set-up and tools that we present in Section 2. The results obtained with this experimental set-up are presented in Section 3. Finally, conclusions are presented in Section 4.

2 MATERIAL AND METHODS

2.1 Experimental set-up

We have chosen to design the active deck as a bridge section model, since it is a standard tool for investigating a bridge section's aeroelastic stability [10]. Moreover, all of the above mentioned research groups conducting wind tunnel experiments have employed bridge section models. We are extending the investigation of active flutter control to bridge section models endowed with multiple flaps, so that the potential of a physically distributed mitigation system can be studied and validated experimentally. The bridge section model is installed in a boundary layer wind tunnel (dimensions: 1.5x2x10 m), as seen in Fig. 3. The test section has a maximal wind speed of 24 m/s. The spring suspended active bridge section model is endowed with 8 flaps, 4 on each of the leading and trailing edge sides. The heave and pitch of the deck as well as the flap positions are communicated at a frequency of 200 Hz. Furthermore, a pull-up mechanism and a system that decouples the heave and pitch of the bridge were designed and installed in order to facilitate system identification, as seen in Figure 4. Note that the decoupling system seen in the figure has not been used for the work presented here, only drag wires are restricting the deck in the horizontal DOF. The design of the section model geometry were mainly influenced by advice given in [1] and [11], and the model dimensions are presented in Table 1. Further details of our experimental set-up and in particular the active bridge

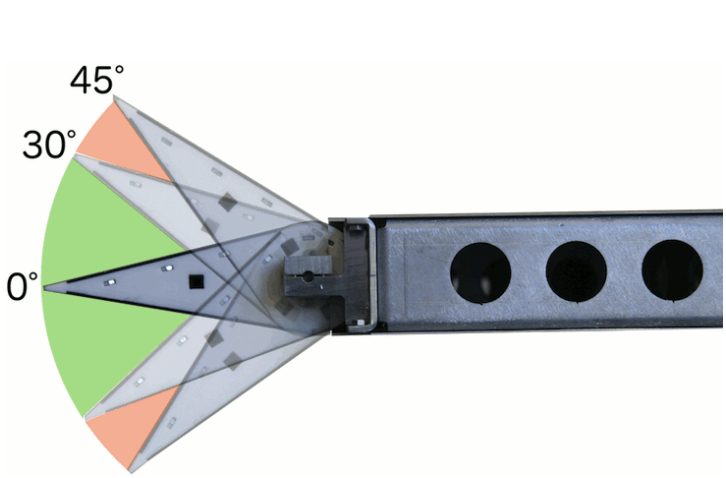

A The normal operating range of the flap lies within the green area. However, during the initial homing, the flap will move into the red area.

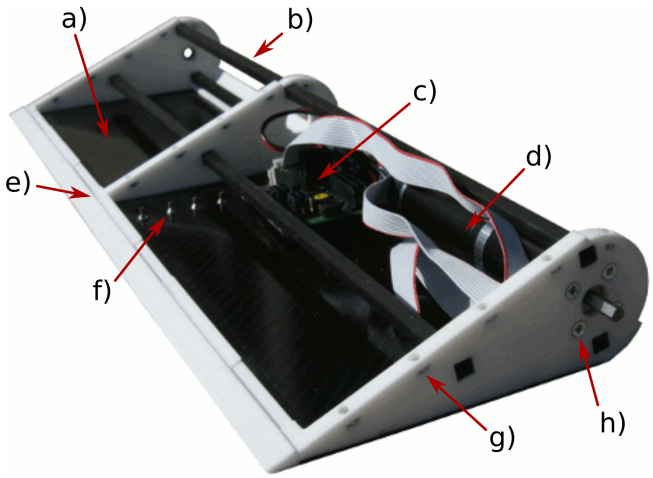

B A flap with the lid removed exposing some key elements of the design: a) carbon fiber sheet, b) carbon fiber rod, c) driver, d) motor, e) 3D printed frame, f) pressure tap, g) nut for attaching the lid, and h) motor anchoring to the frame.

Figure 5: The flap and the attachment to the bridge deck.

section model are presented in [12]. Each flap is attached directly to the deck on hinges and contains its driver and actuator unit, as seen in Figure 5. The design choices, as well as an innovative model-based tuning approach for the position control, for a single flap were presented in [13].

Table 1: Section Model Parameters

Parameter	SmartBridge
Mass, m [kg]	32.3
Mass moment of inertia, I [kgmˆ2]	0.96
Deck width (excl. flaps), B' [mm]	500
Deck width (incl.), B [mm]	740
Deck depth, D [mm]	48
Deck length, L [mm]	1800
Spring constant, k [N/m]	483
Distance between springs, $2a$ [mm]	430
ζ_α	0.018
ζ_h	0.012
ω_α [rad/s]	13.63
ω_h [rad/s]	10.94

2.2 Analytical model of canonical bridge deck

The analytical model of the bridge section model is based on the heave and pitch Degrees of Freedom (DOFs), the fundamental modes involved in coupled flutter. Under the assumption that the bridge deck is symmetric (center of mass and elastic center lie together) the structural dynamics can be modeled as two uncoupled harmonic oscillators in heave and pitch [10]. The model of the external lift and moment caused by the aerodynamic forces on a canonical bridge section model can be estimated with Theodorsen's flutter derivatives [4]. This model baseline, is given by the two-dimensional differential equations below

$$m(\ddot{h} + 2\zeta_h\omega_h\dot{h} + \omega_h^2 h) = L_h = \frac{1}{2}\rho U^2 BK\left[H_1^*\frac{\dot{h}}{U} + H_2^*\frac{B\dot{\alpha}}{U} + KH_3^*\alpha + KH_4^*\frac{h}{B}\right] \quad (1)$$

$$I(\ddot{\alpha} + 2\zeta_\alpha\omega_\alpha\dot{\alpha} + \omega_\alpha^2\alpha) = M_\alpha = \frac{1}{2}\rho U^2 B^2 K\left[A_1^*\frac{\dot{h}}{U} + A_2^*\frac{B\dot{\alpha}}{U} + KA_3^*\alpha + KA_4^*\frac{h}{B}\right] \quad (2)$$

where h and α are the heave and pitch positions, m is the mass of the deck, I is the mass moment of inertia of the deck, ζ_h and ζ_α are the damping ratios in the heave and pitch DOFs, and ω_h and ω_α are their natural circular frequencies, and L_h and M_α are external lift and moment on the deck. Furthermore, ρ is the air density, B is the bridge deck width, U is the wind speed, $K = B\omega/U$ is the reduced frequency, and $H_1^*, ..., H_4^*$ and $A_1^*, ..., A_4^*$ are the non-dimensional flutter derivatives for the deck. The left hand side of the equations represents the structural part of the model and the right hand side the aerodynamic part.

The flutter derivatives can be approximated with the values of a flat plate and are calculated with Theodorsen's circulatory function: $C(K) = F(K) + iG(K)$ [4], as follows [10]

$$
\begin{aligned}
H_1^*(K) &= -\tfrac{2\pi F(K)}{K} \\
H_2^*(K) &= -\tfrac{\pi}{2K}\left[1+\tfrac{4G(K)}{K}+F(K)\right] \\
H_3^*(K) &= -\tfrac{2\pi}{K^2}\left[F(K)-\tfrac{KG(K)}{4}\right] \\
H_4^*(K) &= \tfrac{\pi}{2}\left[1+\tfrac{4G(K)}{K}\right] \\
A_1^*(K) &= \tfrac{\pi F(K)}{2K} \\
A_2^*(K) &= -\tfrac{\pi}{8K}\left[1-\tfrac{4G(K)}{K}-F(K)\right] \\
A_3^*(K) &= \tfrac{\pi}{2K^2}\left[\tfrac{K^2}{32}+F(K)-\tfrac{KG(K)}{4}\right] \\
A_4^*(K) &= -\tfrac{\pi G(K)}{2K}
\end{aligned}
\tag{3}
$$

2.3 Extended model for flap control

In order to consider the external lift and moment caused by the flaps the model can be extended with a modified version of the wing-aileron-tab configuration (transformed into bridge deck with leading and trailing flaps) developed by Theodorsen and Garrick [5], an extension which implies additional flutter derivatives. The lift and moment generated by the leading and trailing edge flaps are directly added to those of the traditional model of a passive deck, i.e., L_h and M_α in Eqs. 1 and 2. Assuming that the flaps move at the same frequency as the deck, they are given by

$$m(\ddot{h}+2\zeta_h\omega_h\dot{h}+\omega_h^2 h) = L_h + L_l + L_t \tag{4}$$

$$I(\ddot{\alpha}+2\zeta_\alpha\omega_\alpha\dot{\alpha}+\omega_\alpha^2\alpha) = M_\alpha + M_l + M_h \tag{5}$$

$$L_l = \frac{1}{2}\rho U^2 BK\left[H_7^*\frac{B\dot{\alpha_l}}{U}+KH_8^*\alpha_l\right] \tag{6}$$

$$M_l = \frac{1}{2}\rho U^2 B^2 K\left[A_7^*\frac{B\dot{\alpha_l}}{U}+KA_8^*\alpha_l\right] \tag{7}$$

$$L_t = \frac{1}{2}\rho U^2 BK\left[H_5^*\frac{B\dot{\alpha_t}}{U}+KH_6^*\alpha_t\right] \tag{8}$$

$$M_t = \frac{1}{2}\rho U^2 B^2 K\left[A_5^*\frac{B\dot{\alpha_t}}{U}+KA_6^*\alpha_t\right] \tag{9}$$

where the additional flutter derivatives due to the flaps, $H_5^*, ..., H_8^*$ and $A_5^*, ..., A_8^*$, are given in the following equations

$$
\begin{aligned}
H_5^*(K) &= \tfrac{1}{2K}\left[T_4 - F(K)T_{11} - \tfrac{4G(K)T_{10}}{K}\right] \\
H_6^*(K) &= \tfrac{1}{K^2}\left[-\tfrac{K^2T_1}{4} - 2F(K)T_{10} + \tfrac{KG(K)T_{11}}{2}\right] \\
H_7^*(K) &= \tfrac{T_4}{2K} \\
H_8^*(K) &= -\tfrac{T_1}{4} \\
A_5^*(K) &= \tfrac{1}{4K}\left[-T_1 + T_8 + cT_4 - \tfrac{T_{11}}{2} + \tfrac{F(K)T_{11}}{2} + \tfrac{2G(K)T_{10}}{K}\right] \\
A_6^*(K) &= \tfrac{1}{2K^2}\left[-T_1 - T_{10} - \tfrac{K^2(T_7+cT_1)}{4} + F(K)T_{10} + \tfrac{KG(K)T_{11}}{4}\right] \\
A_7^*(K) &= -\tfrac{T_1-T_8-cT_4}{4K} \\
A_8^*(K) &= \tfrac{1}{2K^2}\left[-T_4 - \tfrac{K^2}{4}(T_7+cT_1)\right]
\end{aligned}
\tag{10}
$$

where the values for the Theodorsen constants [5], $T_1, T_4, T_7, T_8, T_{10}$ and T_{11} are only depending on the deck and flap dimensions as the value $c = B/B'$, and are calculated as follows

$$\begin{aligned} T_1 &= -\tfrac{1}{3}(2+c^2)\sqrt{1-c^2} + c(cos^{-1}c) \\ T_4 &= c\sqrt{1-c^2} - cos^{-1}c \\ T_7 &= -\tfrac{1}{8}c(7+2c^2)\sqrt{1-c^2} - (\tfrac{1}{8}+c^2)cos^{-1}c \\ T_8 &= -\tfrac{1}{3}(1+2c^2)\sqrt{1-c^2} + c(cos^{-1}c) \\ T_{10} &= \sqrt{1-c^2} + cos^{-1}c \\ T_{11} &= (2-c)\sqrt{1-c^2} + (1-2c)cos^{-1}c \end{aligned} \tag{11}$$

We will investigate the amplitude-gain and phase-shift control law using the bridge deck pitch as input. The leading and trailing edge flaps' positions are calculated accordingly

$$\alpha_l(t) = A_l e^{-i\phi_l}\alpha(t) \tag{12}$$

$$\alpha_t(t) = A_t e^{-i\phi_t}\alpha(t) \tag{13}$$

where A_l and A_t are the amplitude gains, and ϕ_l and ϕ_t are the phase-shifts of the leading and trailing edge flaps respectively.

In order to express the extended system purely in terms of the bridge pitch and heave the Eqs. 1 and 2 are still valid if the flutter derivatives H_2^*, H_3^*, A_2^* and A_3^* are modified appropriately. For the proposed control laws in Eqs.12 and 13 the modified flutter derivatives are given by [6]

$$\begin{aligned} H_2^{*\prime} &= H_2^* + H_5^* A_t cos(-\phi_t) + H_6^* A_t sin(-\phi_t) + H_7^* A_l cos(-\phi_l) + H_8^* A_l sin(-\phi_l) \\ H_3^{*\prime} &= H_3^* - H_5^* A_t sin(-\phi_t) + H_6^* A_t cos(-\phi_t) - H_7^* A_l sin(-\phi_l) + H_8^* A_l cos(-\phi_l) \\ A_2^{*\prime} &= A_2^* + A_5^* A_t cos(-\phi_t) + A_6^* A_t sin(-\phi_t) + A_7^* A_l cos(-\phi_l) + A_8^* A_l sin(-\phi_l) \\ A_3^{*\prime} &= A_3^* - A_5^* A_t sin(-\phi_t) + A_6^* A_t cos(-\phi_t) - A_7^* A_l sin(-\phi_l) + A_8^* A_l cos(-\phi_l) \end{aligned} \tag{14}$$

2.4 Estimating model parameters

In order to estimate the model parameters of the system it is convenient to express Eqs. 1 and 2 in state-space form

$$\dot{Y} = AY \tag{15}$$

where

$$\begin{aligned} Y &= \begin{bmatrix} h \\ \alpha \\ \dot{h} \\ \dot{\alpha} \end{bmatrix} A = \begin{bmatrix} \mathbf{0} & \mathbf{I} \\ (K_{se} - K_s) & (C_{se} - C_s) \end{bmatrix} \\ C_s &= \begin{bmatrix} 2\zeta_h\omega_h & 0 \\ 0 & 2\zeta_\alpha\omega_\alpha \end{bmatrix} K_s = \begin{bmatrix} \omega_h^2 & 0 \\ 0 & \omega_\alpha^2 \end{bmatrix} \\ C_{se} &= \tfrac{1}{2}\rho U B K \begin{bmatrix} H_1^*/m & BH_2^*/m \\ BA_1^*/I & B^2A_2^*/I \end{bmatrix} \\ K_{se} &= \tfrac{1}{2}\rho U^2 K^2 \begin{bmatrix} H_4^*/m & BH_3^*/m \\ BA_4^*/I & B^2A_3^*/I \end{bmatrix} \end{aligned} \tag{16}$$

The system parameters are determined by estimating the matrix A based on the step responses in pitch and heave of the deck (the actual flap positions are thus not considered when performing the parameter estimation). Step responses performed without wind allows the structural model parameters in K_s and C_s to be determined from the obtained matrix A. Step responses performed to the uncontrolled deck with wind present allows the aerodynamic parameters in K_{se} and C_{se}, i.e. the flutter derivatives, to be determined. Additionally, performing the same analysis when the deck is being controlled allows the modified aerodynamic parameters to be obtained, from which the additional flutter derivatives ($H_{5..8}^*$ and $A_{5..8}^*$) can be calculated.

Table 2: Control parameters

Controlled entity	$(A_{L,T})$	$\phi_{L,T}(ms)$	$\phi_{L,T}(Hz)$ at f_α	$\phi_{L,T}(Hz)$ at f_f
Leading flaps	0.5	95	74.2	66.7
Trailing flaps	0.5	340	265.5	238.8

In order to estimate the matrix A, and consequently all model parameters, two different estimation methods have been used; an Eigensystem realization method (EIG) [14] and the Modified Ibrahim Time-Domain (MITD) method [15]. The two methods were compared in order to insure the reliability of the parameter estimations. The EIG method was developed for modal parameter estimation and model reduction for dynamical systems. The MITD method have been widely used for identifying direct and cross flutter derivatives from coupled free vibration experiments. It is important to appropriately assign the values of two time-shift parameters in order to insure the quality, as suggested in [15] we set $N_1 = 1/(4\delta t f_d)$ (where δt is the sampling interval and f_d is the highest modal frequency) and $N_2 = N_1 + 2$.

The data length was set to 800 (i.e., 4 s) for the system identification. The data was filtered with a Butterworth filter with a cut-off frequency at 5.5 Hz. Furthermore, the bias was removed from the step response data (to insure that the heave and pitch oscillate around zero).

3 WIND TUNNEL EXPERIMENTS

3.1 Experimental conditions

In order to extract all the model parameters experimentally we leveraged the pull-up mechanism to do systematic step responses of the deck. The step responses were made by pulling up the windward side of the deck by 30 mm and releasing it, resulting in a mixed step response of the deck in heave and pitch DOFs. The structural model parameters were determined from step responses performed without wind and the aerodynamic parameters from step responses performed at wind speeds ranging between 0 and 12 m/s with increments of 2 m/s.

First, all the model parameters were estimated for the uncontrolled deck (with flaps fixed at a 0°angle). Then, the experiments were repeated for three different active control strategies: control using all flaps, control using only leading flaps (all the trailing flaps were fixed to a 0° angle), and control using only trailing flaps (all the leading flaps were fixed to a 0° angle). By introducing the leading and trailing edge flap control incrementally the complexity of the system was slowly increased.

In order to estimate the mechanical and aerodynamic model parameters, a total of 140 step responses in the wind tunnel were performed (7 wind settings x 4 control types x 5 runs per setting).

The control parameters, i.e., the phase-shifts and amplitude gains, were manually tuned so that flutter would still occur when all flaps were used for the control. Thus the control parameters were purposely not chosen to be efficient at suppressing flutter, but rather to provide usable data for parameter estimation of the system.

The parameters implemented for the experiments are found in Table 2. Note that the phase-shifts were implemented as time delays in the controller, which has the effect that the phase-shift in terms of frequency is depending on the frequency of the control input signal, i.e. the pitch. Since the pitch frequency lies between the natural frequency, f_α, and the flutter frequency, f_f, the actual phase-shifts lie between the limits given in Table 2. Therefore, in the following analysis of the experimental data the phase-shifts are not constants but calculated from the pitch frequency.

The leading and trailing flap responses to the deck pitch motion during a step response without wind is shown in Fig. 6, where the phase-shifts are clearly detectable. However, there is a clear deviation (jerk) from the desired trajectory for the trailing flap at approximately 0.7 s. This type of behavior has been noted, sometimes for the leading flaps too, but more often for the trailing flaps, in all the controlled experiments, and seems to be a set-point communication issue for the local bus of our system (in fact, the trailing flap appears to receive the wrong set-point). Note that these deviations have not been accounted for in the parameter estimations presented here since the actual flap trajectories are not used in the parameter estimation, thus the effects of a sporadic jerk of a flap is assumed to be negligible. Whether this assumption holds will be tested experimentally as soon as the communication issue in our set-up has been addressed.

3.2 Experimental results

The resulting step responses for the entire range of wind speeds for the uncontrolled deck are shown in Fig. 7. It is evident that the system damping and frequencies for both the heave and pitch are dependent on the wind speed. The flutter wind speed of the uncontrolled deck was determined experimentally to be 9.3 m/s, at higher wind speeds the flutter develops more rapidly.

The resulting step responses for all the different control configurations without wind are shown in Fig. 8. In theory, the step responses performed without wind should be identical for all the control cases since the inertial forces of the flaps are neglected in our model. Generally, the experiments support that this is a fair assumption, at least when considering the frequencies of the system and the damping in the heave DOF. However, the damping in the pitch is slightly affected by the flap motions when there is no wind present. Furthermore, it is curious that the leading and trailing flaps have an asymmetric effect on the bridge pitch damping, were in theory the motion of the flaps on only one side of the deck should have the same effect independent of the side being controlled. This could be due to eccentricities in our set-up or possibly due to the jerky behavior of the flaps (an effect which is not symmetric, the trailing flaps are affected to a larger extent by this issue). However, the cause of the asymmetric output has not yet been determined and need to be investigated further.

The resulting step responses for all the different control configurations with a 10 m/s wind are shown in Fig. 9, where it is clear that

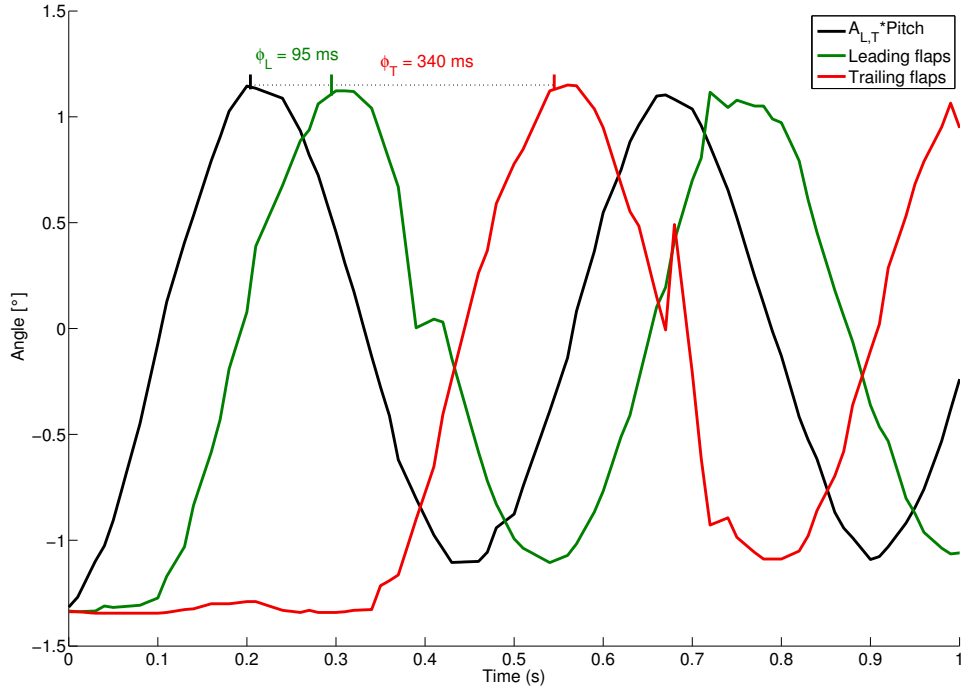

Figure 6: Leading and trailing flaps trajectories at 0 m/s. The trajectories of the leading and trailing flaps are reported by the motor encoders, while the pitch is given by the laser measurements. The pitch is scaled by the amplitude gain of the control in the graph.

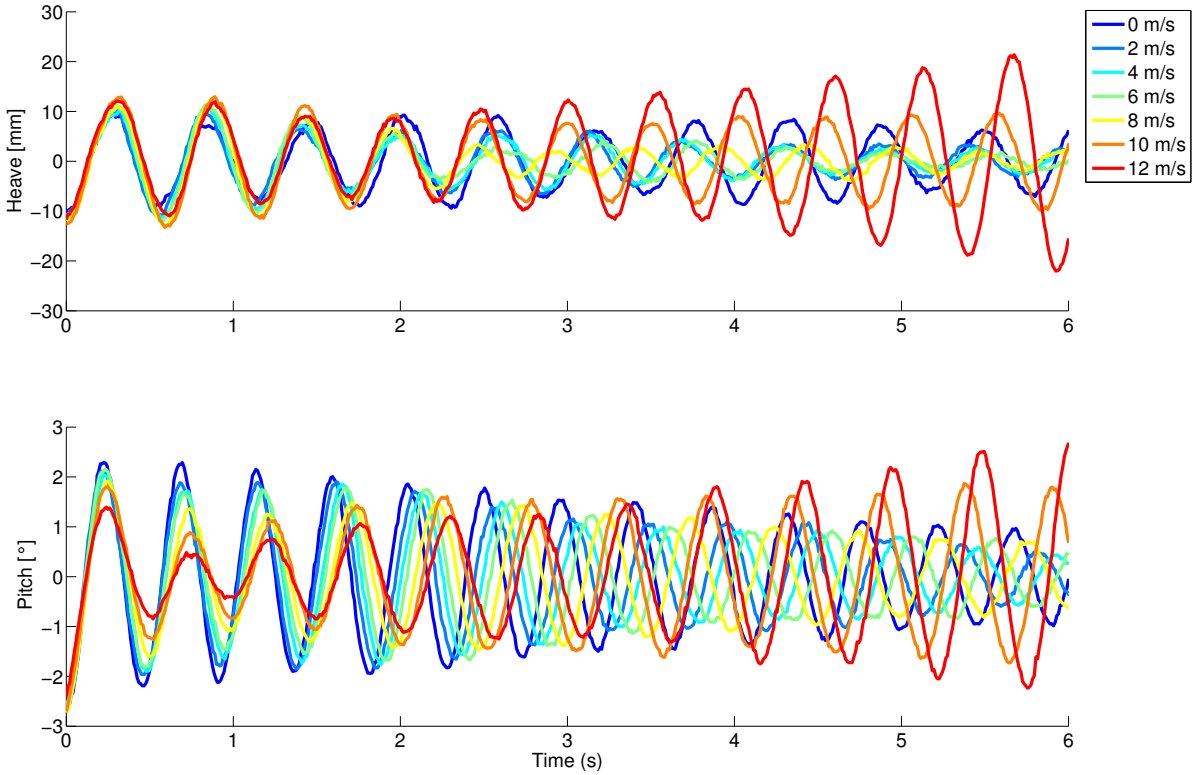

Figure 7: Step responses of the uncontrolled deck at varying wind speeds.

using all flaps for the control is more efficient than using flaps only on a single edge. However, there does not seem to be a significant difference between using only flaps on the leading edge or only on the trailing edge in this case.

The result of the estimated flutter derivatives for the uncontrolled deck using the EIG and MITD methods are presented in Fig. 10 as well as the corresponding theoretical values. Generally the two methods produce similar results, with a good agreement with the theoretical values (except for H_4^*) for the direct flutter derivatives in Fig. 10A, and a fair agreement with the theoretical values for the cross flutter derivatives in Fig. 10B. It is expected that the identified parameters will diverge from the theoretical ones, since in fact our bridge deck is not a flat plate.

For the parameter estimations presented from here on we only used the EIG method, it was chosen because the overall agreement with the theoretical values appear better, however, this is not a clear case.

The mean values of the estimated flutter derivatives for all control cases are given in Fig. 11. Note that according to the theoretical model H_1^*, H_4^*, A_1^*, and A_4^* should be unaffected by the flap control, while $A_2^{*'}$, $A_3^{*'}$, $H_2^{*'}$, and $H_3^{*'}$, are functions of the corresponding uncontrolled deck derivatives (A_2^*, A_3^*, H_2^*, and H_3^*) as well as the leading and trailing flap derivatives ($H_{5..8}^*$ and $A_{5..8}^*$) as described in Eqs. 14. However, our experimental results show a significant difference in the estimates of the flutter derivatives that theoretically should be independent of flap control. Generally, these derivatives are estimated similarly independently of the active control type, but is significantly different from the uncontrolled case. The clearest example being the H_1^* derivative, where the uncontrolled deck differ significantly from the estimations with control, independent of the control type (trailing, leading, or all flaps). The same tendency is observed for A_1^*, and to some extent A_4^* and H_4^* (however here the leading edge compares well to the estimates for no control, although the estimations are scattered).

The flutter derivatives that theoretically should be dependent on the control, i.e., $A_2^{*'}$, $A_3^{*'}$, $H_2^{*'}$, and $H_3^{*'}$, are also so in our experiments. However, there is no consistent trend compared to the theoretical derivatives. The tendency for the different controls of the $A_2^{*'}$ estimate are similar to those in theory; the trailing flap control and no control are similar, and distinguishable from the leading flap control and the control using all flaps, which are also similar. In contrast, all the $H_3^{*'}$ and $A_3^{*'}$ estimations for active controls (independent of type) yields similar estimations, and distinguishable from the uncontrolled deck, when in theory controlling only the leading flaps should produce a result similar to the uncontrolled deck. The estimations of $H_2^{*'}$ are quite scattered at higher wind speeds. However, the tendency seems to be that having no control or using all flaps in the control yield similar estimates, and using only one side for control, either on the trailing or leading edge, yield similar result, while in theory using only the leading side should be close to using no control.

The estimations of flutter derivatives for the trailing flap control, in Fig. 11, seem to be the least consistent, which could be due to the prominent jerky flap behavior in this control type. However, overall the tendencies of these flutter derivatives are consistent with those of the leading flap. Since this control type only had minor disruptions of the flap actuation, it would suggest that the results obtained from control with the trailing flap (and using all flaps) are only marginally influenced by the disturbances in the actuation.

The flutter derivatives for the leading and trailing flaps can be indirectly obtained from the results presented in Fig. 11, according to Eqs. 14, these indirect estimations are presented in Fig.12. The results in Fig. 12A were obtained from the estimations made with control using only the leading flaps, and the results in Fig. 12B were obtained from the estimations gathered with control using only the trailing flaps. In both cases the estimated derivatives are scattered. Further investigations need to be made in order to tell whether this is due to noise, estimation procedure, or incorrect model assumptions.

Interestingly, the obtained flutter derivatives for the leading and trailing flaps compare similarly to the expected theoretical values, which would suggests that the jerking behavior in the flap actuation of the trailing flaps do not have a too grave impact on the system behavior.

Note that the flap flutter derivatives also can be estimated directly using the flap trajectories, which would imply extending the Y vector and estimating a larger A matrix in Eqs. 15 and 16. The authors intend to conduct such analysis for the continuing investigation of the work presented here.

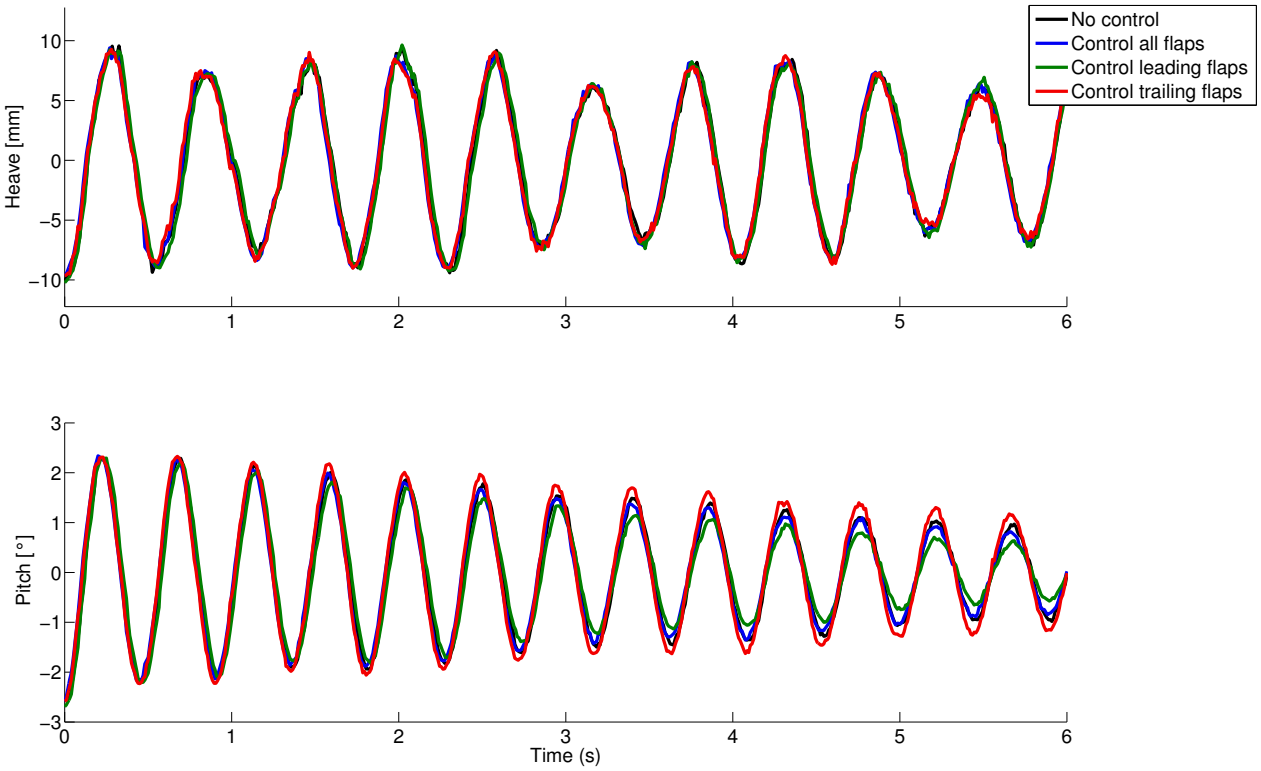

Figure 8: Uncontrolled vs. controlled deck step response 0 m/s.

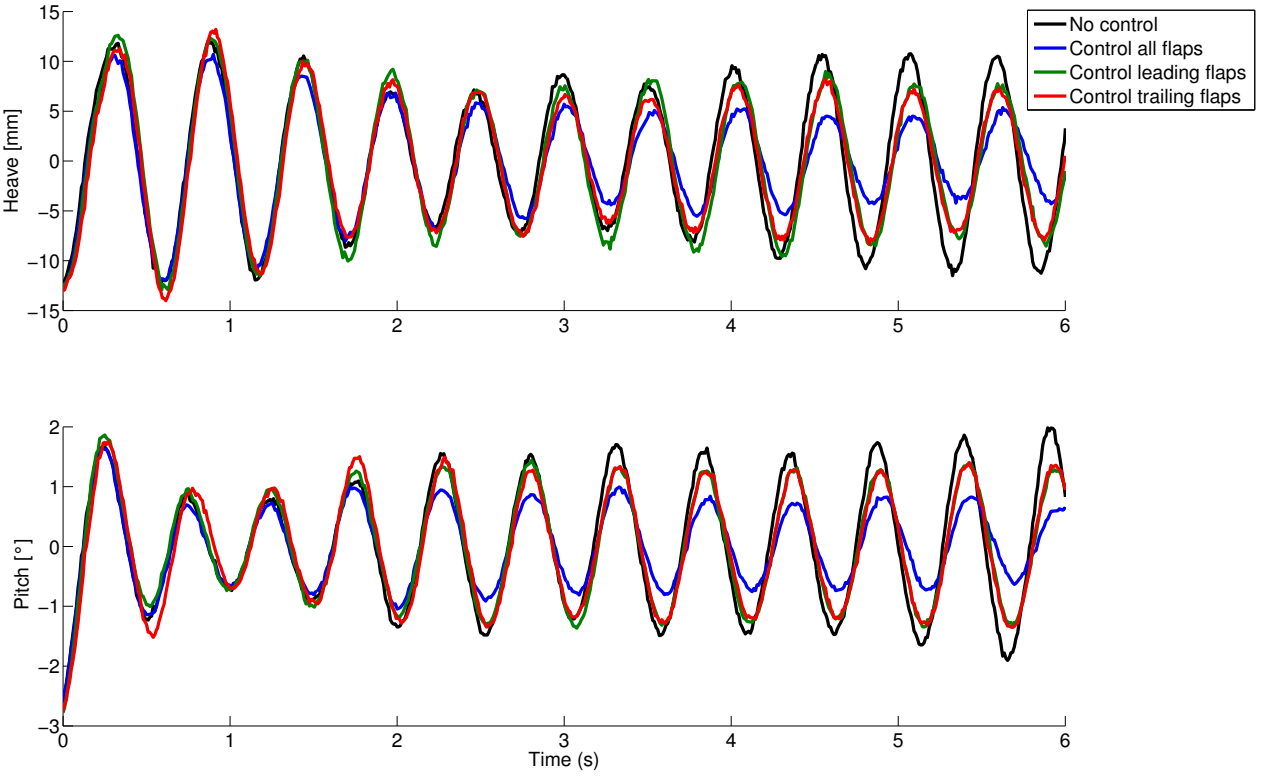

Figure 9: Uncontrolled vs. controlled deck step response 10 m/s.

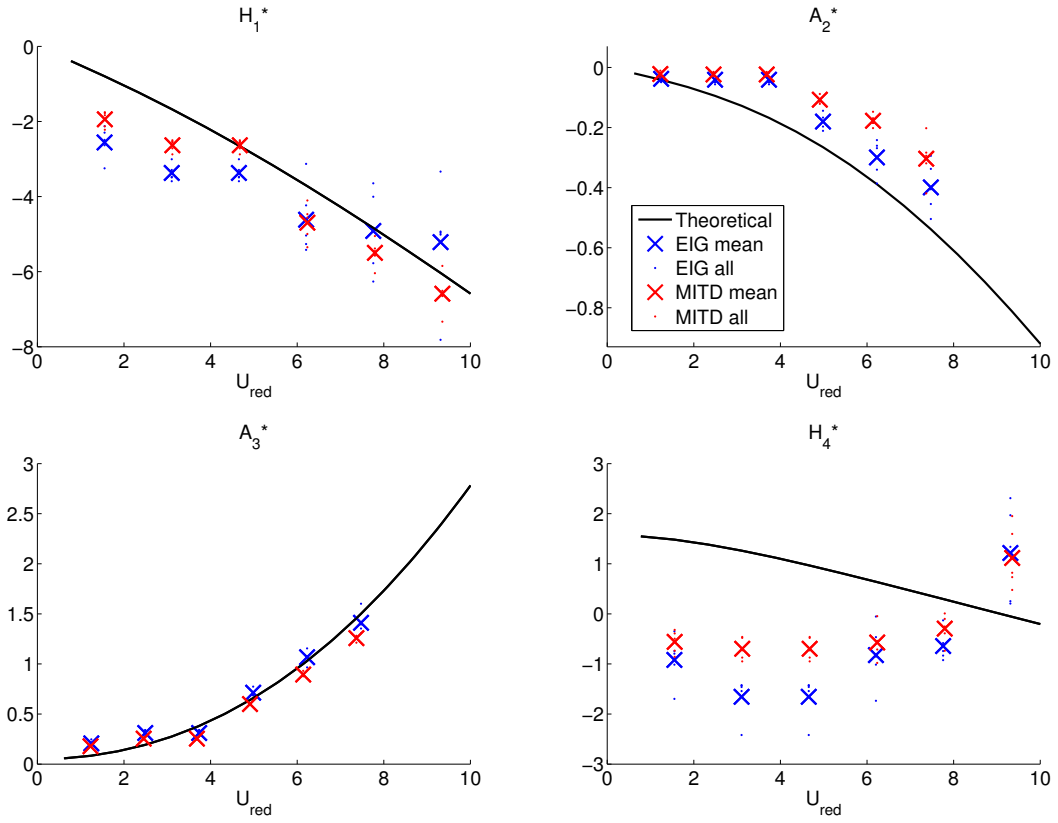

A Direct flutter derivatives.

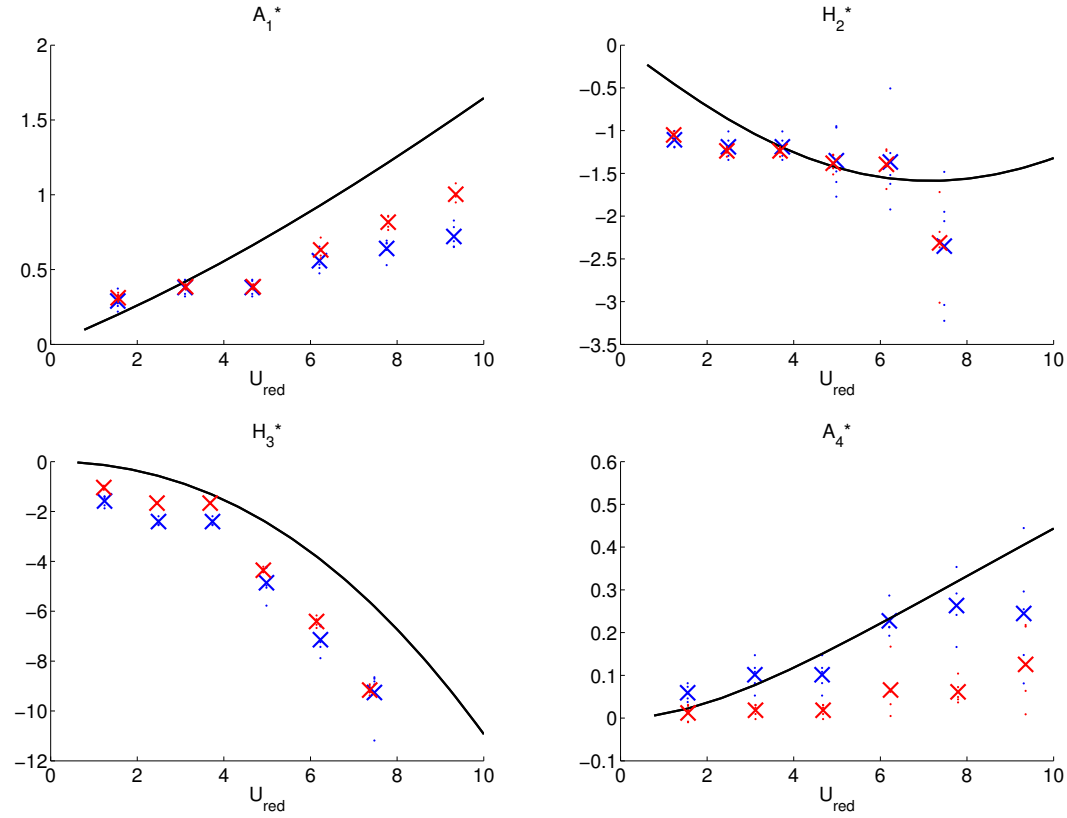

B Cross flutter derivatives.

Figure 10: Identified flutter derivatives for the uncontrolled deck using different estimation methods.

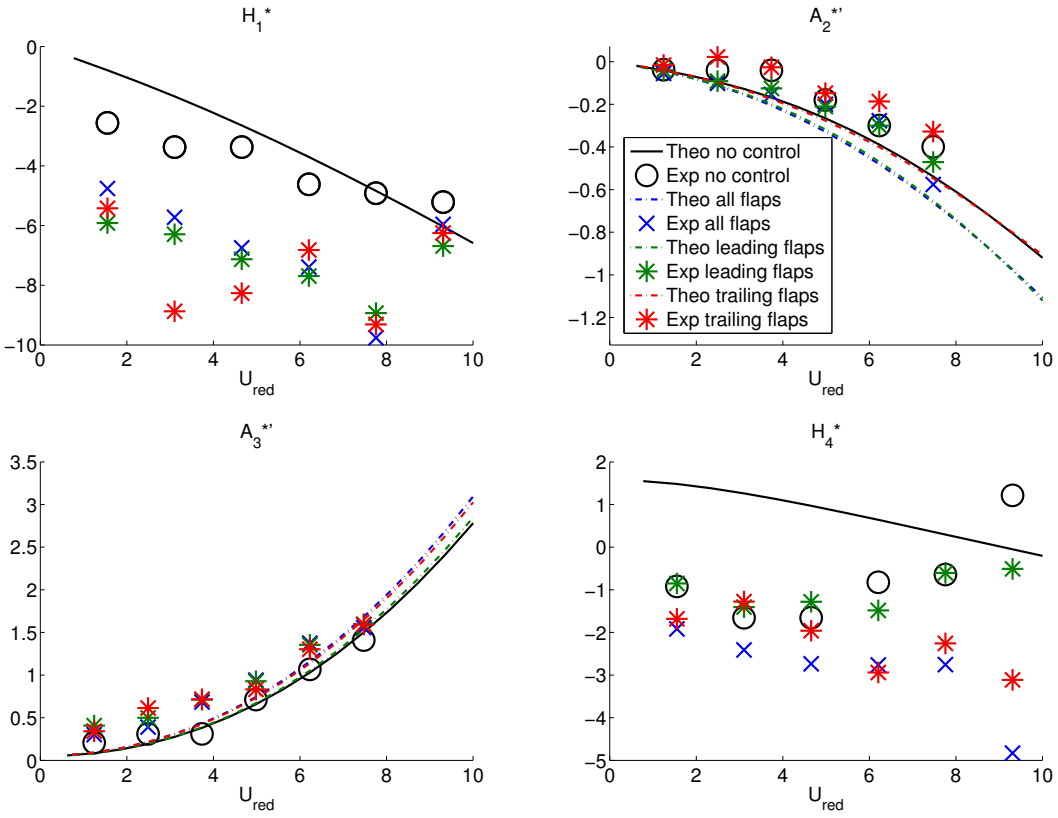

A Direct (modified) flutter derivatives.

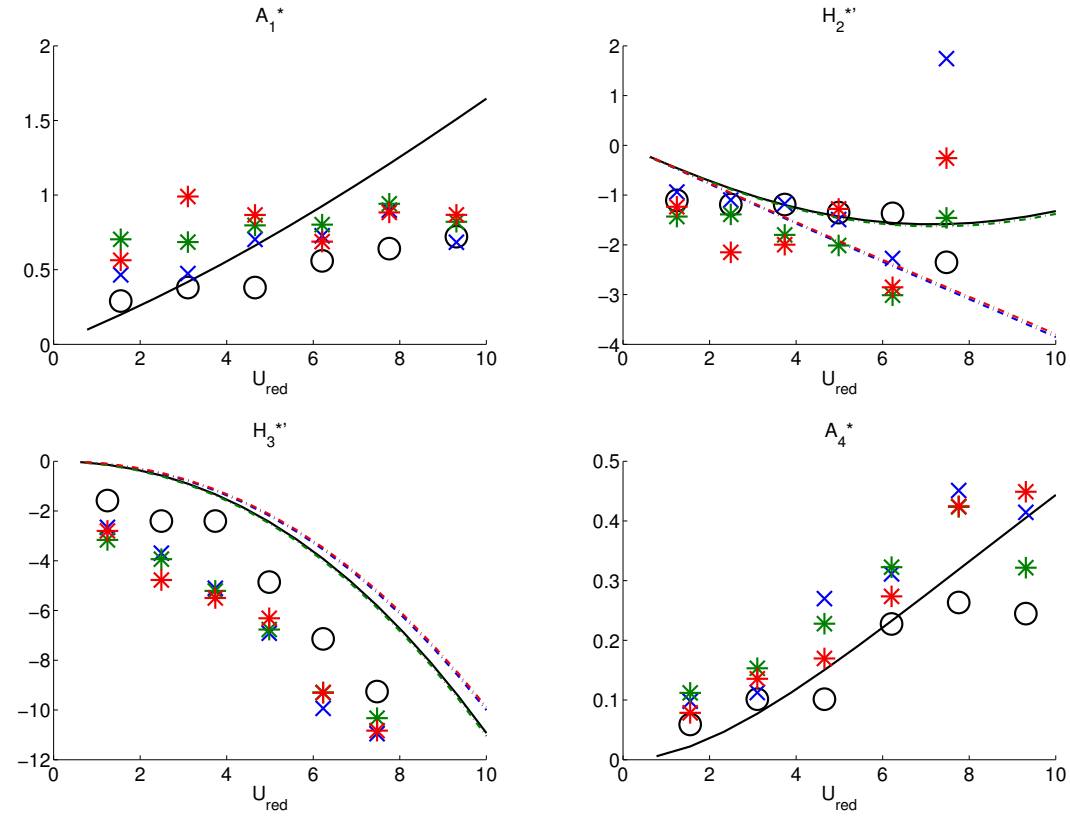

B Cross (modified) flutter derivatives.

Figure 11: Identified flutter derivatives for the different control cases, using only the EIG method.

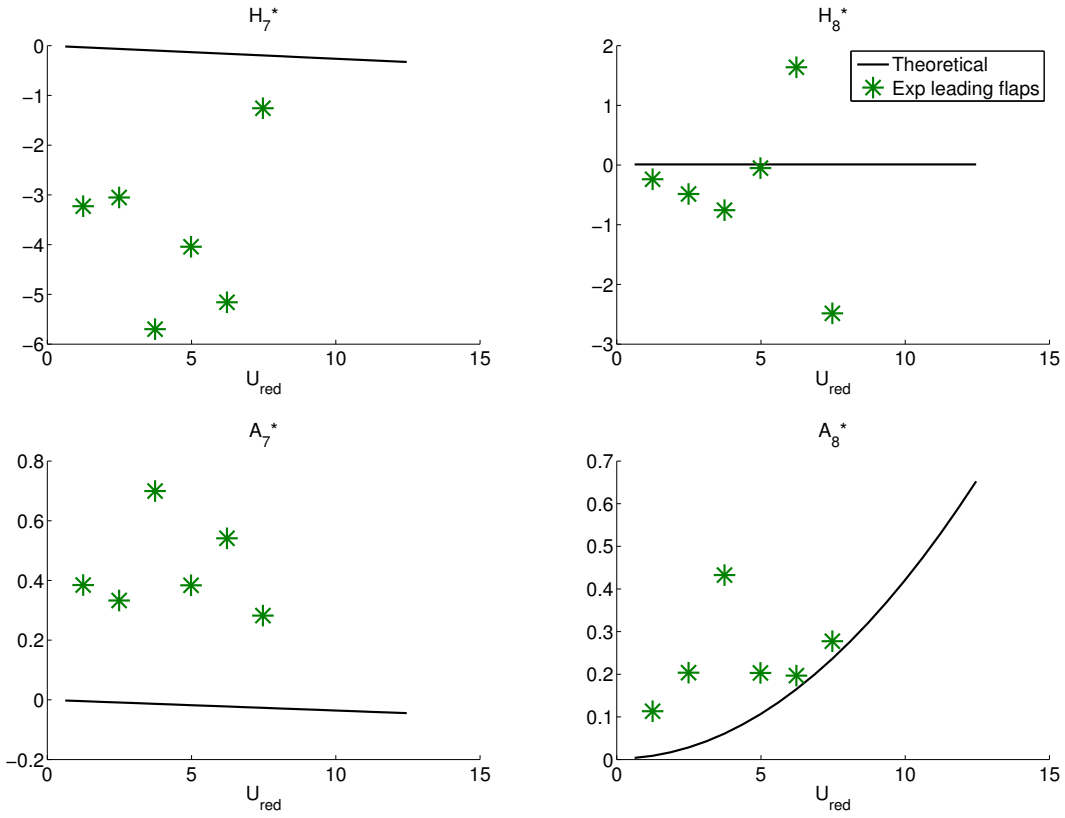

A Leading flap flutter derivatives, identified from the leading flap only control case.

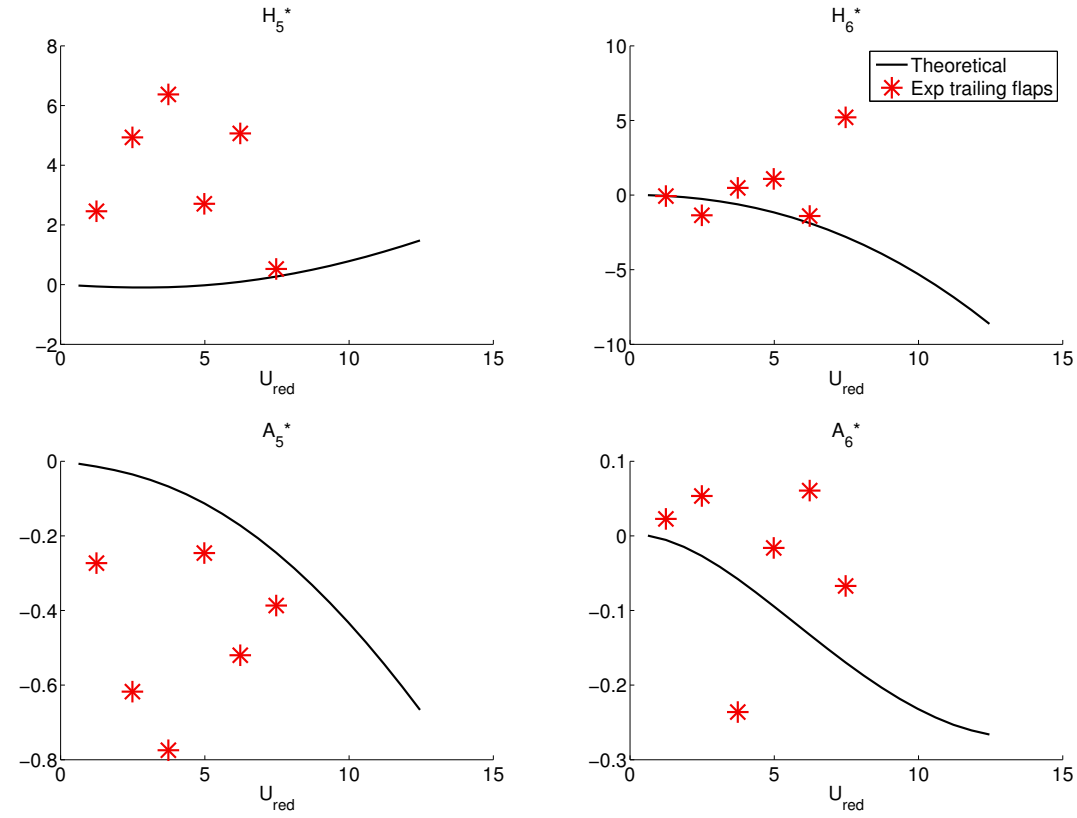

B Trailing flap flutter derivatives, identified from the trailing flap only control case.

Figure 12: Identified additional flutter derivatives for the leading and trailing flaps (from EIG system identification).

4 CONCLUSIONS

In this work, we aim to thoroughly investigate the applicability of the wing-aileron-tab combination to a bridge deck equipped with moving leading and trailing edge flaps. We employed a systematic approach in order to estimate all the model parameters with wind tunnel experiments, leveraging our unique set-up.

We estimated model parameters from a total of 140 step responses for four different control strategies: using no control, only leading flaps, only trailing flaps, and using all flaps. To the best of the authors knowledge, this is the first presentation of experimentally extracted flutter derivatives from a bridge deck with active flap control.

We show that the flutter derivatives that in theory should be unaffected by flap motion, clearly deviate between the controlled and uncontrolled case for the experimentally extracted derivatives. A result that would suggest that the wing-aileron-tab model is not capturing the real dynamics.

Furthermore, the additional flutter derivatives due to the leading and trailing edge flaps are indirectly estimated. Although, the results are quite scattered, they mostly lie within an acceptable region of the theoretical values. The next step will be to compare these indirect estimations to the derivatives estimated directly using the flap trajectory data.

In summary, we have made significant progress in the investigation of the applicability of the wing-aileron-tab model applied to a bridge controlled with flaps. The work presented here will be continued in terms of further analysis and experimentation in order to fully evaluate the model's applicability.

REFERENCES

[1] A. Larsen, *Aerodynamics of Large Bridges*. Taylor & Francis, 1992.

[2] H. Kobayashi and H. Nagaoka, "Active control of flutter of a suspension bridge," *Journal of Wind Engineering and Industrial Aerodynamics*, vol. 41, no. 1–3, pp. 143–151, 1992.

[3] H. Kobayashi, R. Ogawa, and S. Taniguchi, "Active flutter control of a bridge deck by ailerons," in *Second World Conference on Structural Control*, 1998, pp. 1841–1848.

[4] T. Theodorsen, "General theory of aerodynamic instability and the mechanism of flutter," *NACA Tech. Rep. no. 496*, 1935.

[5] T. Theodorsen and I. E. Garrick, "Nonstationary flow about a wing-aileron-tab combination including aerodynamic balance," *NACA Tech. Rep. no. 736*, 1942.

[6] H. I. Hansen and P. Thoft-Christensen, "Active flap control of long suspension bridges," *Journal of Structural Control*, vol. 8, no. 1, pp. 33–82, 2001.

[7] K. Wilde, Y. Fujino, and T. Kawakami, "Analytical and experimental study on passive aerodynamic control of flutter of a bridge deck," *Journal of Wind Engineering and Industrial Aerodynamics*, vol. 80, no. 1 - 2, pp. 105 – 119, 1999.

[8] U. Starossek and H. Aslan, "Passive control of bridge deck flutter using tuned mass dampers and control surfaces," in *Proc., Eurodyn*, 2008, pp. 7–9.

[9] S.-D. Kwon, M. S. Sungmoon Jung, and S.-P. Chang, "A new passive aerodynamic control method for bridge flutter," *Journal of Wind Engineering and Industrial Aerodynamics*, vol. 86, no. 2-3, pp. 187 – 202, 2000.

[10] E. Simiu and R. H. Scanlan, *Wind Effects on Structures: Fundamentals and Application to Design*. New York: John Wiley & Sons, 1996.

[11] M. Matsumoto, K. Mizuno, K. Okubo, and Y. Ito, "Torsional flutter and branch characteristics for 2-d rectangular cylinders," *Journal of Fluids and Structures*, vol. 21, no. 5 - 7, pp. 597 – 608, 2005.

[12] M. Boberg, G. Feltrin, and A. Martinoli, "A novel bridge section model endowed with actively controlled flap arrays mitigating wind impact," in *Robotics and Automation (ICRA), 2015 IEEE International Conference on*, May 2015.

[13] ——, "Model and control of a flap system mitigating wind impact on structures," in *Robotics and Automation (ICRA), 2014 IEEE International Conference on*, May 2014, pp. 264–269.

[14] J. N. Juang and R. S. Pappa, "An eigensystem realization algorithm for modal parameter identification and model reduction," *Journal of Guidance, Control, and Dynamics*, vol. 8, no. 5, pp. 620 – 627, 1985.

[15] P. Sarkar, *New Identification Methods Applied to the Response of Flexible Bridges to Wind*. Johns Hopkins University, 1992. [Online]. Available: https://books.google.ch/books?id=c5wxnQEACAAJ